Microstructural Features of Rolled Mg-3Al-1Zn

M.R. BARNETT, Z. KESHAVARZ, and M.D. NAVE

The microstructures of hot- and cold-rolled Mg-3Al-1Zn (AZ31) are examined using scanning electron and optical microscopy. It is shown that the microstructures following multipass hot rolling and annealing are more uniform than those formed by heavy single pass rolling and annealing. The importance of twins in producing intragranular recrystallization is evident, although the most dominant nucleation site is grain boundaries. The cold-rolled structure after a rolling reduction of 15 pct is dominated by the presence of deformation twins. Twin trace analysis suggests that approximately two thirds of the twins are a form of "*c*-axis compression" twin. A number of "*c*-axis tension" twins were also observed and additional *in-situ* scanning electron microscopy experiments were performed to confirm earlier observations that suggest these twins can form after deformation, during unloading.

I. INTRODUCTION

THE microstructure of rolled magnesium alloys, as in many other metals, exerts a significant influence over mechanical behavior both during processing and in service. As early as 1939, Menzen[1] interpreted the favorable mechanical properties seen in certain wrought alloys to be a consequence of microstructure (grain size) rather than a direct effect of alloy composition. In that work, the improved rolling performance of extruded slab over cast slab was also ascribed to microstructural changes. Couling *et al.*,[2] along with Reed-Hill (in a comment attached to Couling *et al.*'s work) have rationalized the superior cold rollability of Mg-0.5Th and Mg-0.4Zr-0.2 (Misch metal) alloys in terms of the appearance of banded microstructural features ("compression bands" in Roberts' terminology[3]). Deformation twinning also plays a significant role in the development of rolled structures,[4,5,6] and a double-twinning mechanism in which $\{10\bar{1}2\}$ twinning occurs within the interior of $\{10\bar{1}1\}$ twins has been observed in pure Mg.[2,3] The present work examines the microstructural phenomena evident in hot- and cold-rolled commercial quality Mg-3Al-1Zn (AZ31), the most common wrought magnesium alloy.

After hot rolling, the grain size of AZ31 is generally of the order of 10 to 40 μm,[7,8,9] with sizes closer to $\sim$5 μm reported in some instances.[10,11] If the grain size of the AZ31 billet received for use in the present work ($\sim$380 μm) is typical (and our experience suggests that it is), grain refinement by a factor of 10 to 80 times commonly occurs during hot rolling. The hot rolling process involves multiple cycles of rolling followed by reheating, and in a number of Mg alloys it has been reported that even finer structures can be achieved if a small number of high strain rolling passes are used.[12,13] This approach is obviously restricted by the capacity of the rolling mill, but it is also limited by the homogeneity of the structure.[13] With fewer rolling passes, there are fewer cycles of annealing and this is expected to accentuate the effect of the inhomogeneity of the deformed structure on the final recrystallized structure. Optimized hot rolling microstructures can thus be considered to be a trade-off between grain refinement and microstructure homogeneity. Steps toward determining optimal hot rolling parameters are taken in the present work.

Turning to cold rolling, early studies showed ubiquitous diagonally inclined banded features containing basal planes closely aligned with the band.[3] These basal planes are aligned close to 45 deg to the normal (loading) direction and are therefore favorably aligned for slip. Recently, two of the present authors reported electron backscatter diffraction (EBSD) measurements made on cold-rolled samples of pure Mg[6] that were consistent with these observations. It has been suggested that these bands are actually twins in which slip has concentrated.[2] However, in our previous study,[6] we saw no strong evidence for this and opted to refer to the bands as shear bands, due to the similarity of their appearance to shear bands seen in other systems. This is not to say, however, that twinning is not involved in the early stages of their formation, and in the present work, we show that this may well be the case in cold-rolled AZ31.

The mechanism of double twinning, in which $\{10\bar{1}2\}$ twins form in the interior of $\{10\bar{1}1\}$ twins, has received considerable attention in single-crystal and pure Mg literature,[14,15] particularly in regard to the formation of compression bands.[3] In our previous EBSD analyses, we observed boundaries with misorientation angles and axes consistent with the operation of this mode in pure Mg.[16] However, in general, identification of these twins by EBSD analysis was hampered by the difficulty in obtaining diffraction patterns from the interiors of twins suspected to be of this type. In the present work, we obtain the likely identity of twins using trace analysis based on the orientation of the neighboring matrix, which is far more readily obtained using EBSD.

An additional issue that has arisen in the interpretation of the twining modes active in rolled magnesium alloys is the appearance of $\{10\bar{1}2\}$ twins in grains oriented for c-axis *compression*.[6] This twinning mode only permits *extension* along the *c*-axis direction.[17] The phenomenon may well arise from twinning during unloading, something that has been reported to occur when a single crystal of pure Mg was

M.R. BARNETT, QEII Research Fellow, Z. KESHAVARZ, Ph.D. Student, and M.D. NAVE, Postdoctoral Research Fellow, are with the School of Engineering, Deakin University, Geetong VIC 3217, Australia. Contact e-mail: barnettm@deakin.edu.au

This article is based on a presentation made in the symposium entitled "Phase Transformations and Deformation in Magnesium Alloys," which occurred during the Spring TMS meeting, March 14–17, 2004, in Charlotte, NC, under the auspices of ASM-MSCTS Phase Transformations Committee.

unloaded following compression in vice.[14] The possibility that this occurs in AZ31 is examined here by combining twin observations in rolled plate with *in-situ* tensile experiments.

II. EXPERIMENTAL

Two samples of Mg-3Al-1Zn were received for use in this work. One was in the form of rolled plate, 12 mm in thickness, and the other was in the form of cast extrusion billet. The grain sizes for the two samples were approximately 15 and 380 μm, respectively. The rolled plate was strongly textured with a typical sheet basal texture, whereas the cast sample was randomly textured (Figure 1).

Two rolling experiments were conducted. In the first, four different hot rolling schedules were employed to achieve a total rolling strain of 0.7. This experiment was carried out for both the cast material and the rolled plate. Schedule 1 involved rolling pass strains of 0.12; schedule 2, rolling pass strains of 0.24; schedule 3, rolling pass strains of 0.35; and schedule 4 involved a single pass. Prior to rolling, the samples were homogenized for 8 hours at 400 °C. Following each pass, the samples were annealed for 15 minutes at 400 °C. Rolling was carried out at temperatures between 150 °C and 400 °C at an average strain rate of the order of 0.1 s^{-1} (estimated using the equation given in Reference 18). Samples were cooled in air both following rolling and following heat treatment. Prior to rolling, the samples were held at the rolling temperature for 15 to 30 minutes. In the second experiment, the as-received plate was cold rolled to a thickness reduction of 15 pct in passes of ~1 pct each (roll diameter ~400 mm).

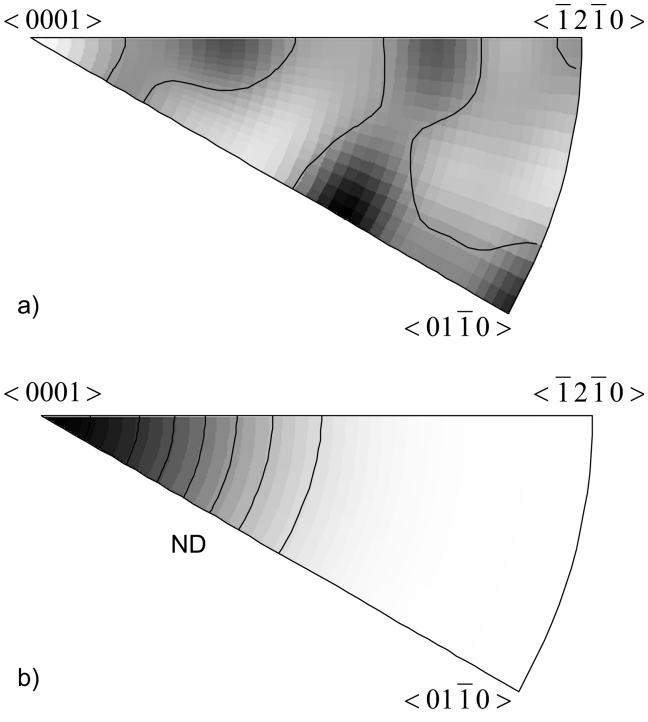

Fig. 1—Inverse pole figures of the starting material measured using EBSD showing (*a*) an arbitrarily chosen direction for one of the batches of cast material (~50 grains) and (*b*) the rolling normal direction for the as-received plate sample (>200 grains). Contour lines 1, 2, 3 . . . times random.

Following the mechanical treatments, samples were prepared for optical and electron microscopy. For the former, samples were mechanically polished down to 1-μm diamond suspension chemical by polished in Nital and then etched. For the latter, mechanical grinding was followed by diamond and colloidal silica polishing. Samples were then etched for ~10 seconds in a solution of 5 pct (by volume) nitric acid, 15 pct acetic acid, 20 pct water, and 60 pct ethanol.[19] Lineal intercept grain sizes were measured and point counting was employed to determine the fraction of recrystallization.

A flat tensile specimen was cut from the cast material for *in-situ* observation of twinning. The sample had a cross section of 10 mm^2 and a gage length of 25 mm. The surface was prepared for EBSD mapping, as described previously. Tensile testing was carried out using an *in-situ* tensile stage in a field emission gun scanning electron microscope. The deformation was performed at ~0.5 μm/s.

III. RESULTS

A. *Hot Rolling*

The microstructures obtained using the cast starting material varied in their degree of homogeneity far more than those seen in the plate starting material. The inhomogeneity seen after rolling the cast starting material can be ascribed to incomplete recrystallization. This interpretation is based on the identification of unrecrystallized regions characterized by (1) a grain size similar to the starting grain size, (2) grains elongated in the rolling direction, and (3) the presence, in some cases, of an internal structure of large twins or banded features decorated by recrystallized grains. Examples of unrecrystallized structures are shown in Figure 2. For the cast samples, the fraction recrystallized was estimated using a point counting method and the results are shown in Figure 3. Lower rolling temperatures and increased numbers of passes lead to higher recrystallized fractions.

The microstructures of the plate samples appeared to be completely recrystallized. Some examples are shown in Figure 4 along with a completely recrystallized structure obtained for the cast starting material. The average lineal intercept in the rolled plate samples is plotted against rolling temperature in Figure 5. Also shown in this plot are the average recrystallized grain sizes seen in the cast samples rolled according to schedule 1. In general, decreasing the reduction per pass served to increase the final grain size. This effect is most noticeable for rolling at higher temperatures in the plate samples. Interestingly, the final grain sizes in the cast samples were finer than the plate specimens under conditions of low pass strain, particularly at higher temperature.

B. *Cold Rolling*

The microstructure of the AZ31 plate after cold rolling to 15 pct thickness reduction is shown in Figure 6. The structure is revealed by assigning a gray scale to the sharpness of the Kikuchi bands obtained during electron backscatter diffraction. (This parameter is commonly termed "band contrast" and is determined automatically by the commercial EBSD software.[20]) The Kikuchi band contrast reflects the

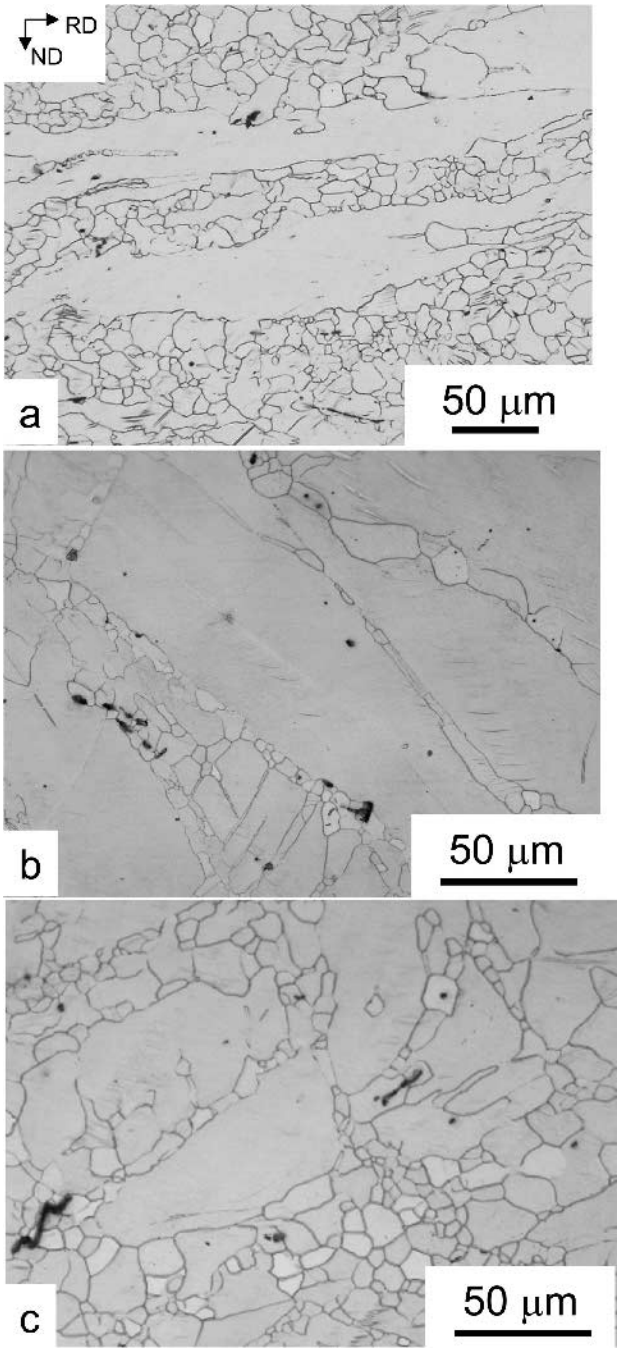

Fig. 2—Partially recrystallized structures of the cast starting material rolled to a total strain of 0.7 in (*a*) two passes at 400 °C, (*b*) one pass at 350 °C, and (*c*) one pass at 400 °C. Each pass was followed by annealing at 400 °C for 15 min (RD-ND section, rolling direction parallel to scale marker).

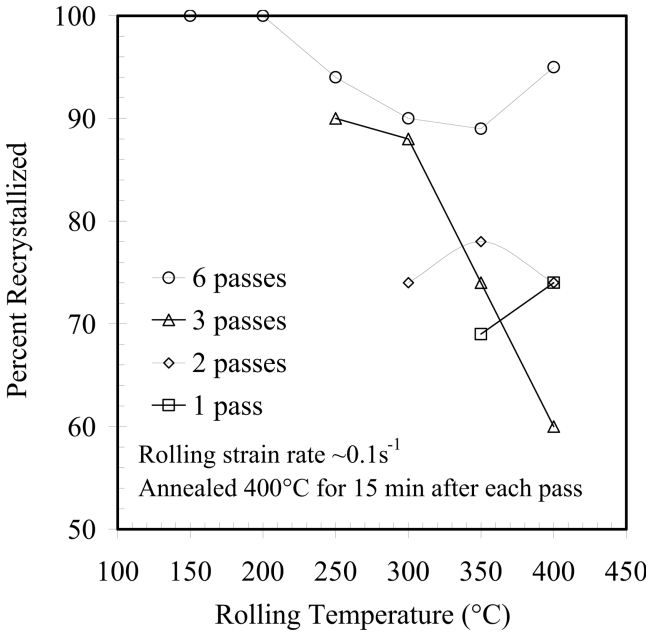

Fig. 3—Influence of rolling temperature on the fraction recrystallized evident in the cast starting material following rolling and annealing. All samples were rolled to a total strain of 0.7.

degree of perfection of the lattice within the backscatter electron interaction volume. In Figure 6, the dark regions correspond to areas of poor lattice perfection, and consequently, grain boundaries and regions of high dislocation density appear dark. This form of imaging is quite useful in the examination of the structures of cold-deformed Mg alloys, in which the indexing of the EBSD pattern is often quite difficult. A Kikuchi band contrast image requires only that EBSD patterns are produced; it does not depend upon the indexing of the pattern.

One of the most obvious features of this micrograph is the presence of twins. The heavy shear or compression bands observed in other studies (*e.g.*, References 2, 3, and 6) are not present in large numbers. This is probably due to the low level of rolling strain used here. A number of dark regions are evident in Figure 6 (*e.g.*, below "36" and above and to the right of "11"), which are presumably regions of high dislocation density and which may represent the early stages of the formation of these bands. Very few of the twin interiors were able to be indexed and we assume that the dark linear features that bisect many of the grains are actually thin twins. The double twinning mechanism discussed previously, in which $\{10\bar{1}2\}$ twins form within a $\{10\bar{1}1\}$ twin, is expected to give rise to boundaries characterized by a 38 deg rotation around a $<11\bar{2}0>$ direction (assuming the plane of shear is shared). Of the twins that were able to be indexed, a few were surrounded by boundaries within 5 deg of this ideal rotation (Figure 7). In the cases shown in Figure 7, the twins are nearly parallel to a $\{10\bar{1}1\}$ plane. These twins are consistent with $\{10\bar{1}1\}/\{10\bar{1}2\}$ double twins.

To establish the degree to which the numerous unindexed twins present in Figure 6 were of this type, trace analysis was carried out. Identification of the double twinning mechanism mentioned previously is not as straightforward as it might seem. The strain and accommodation kinks associated with the secondary "internal" $\{10\bar{1}2\}$ twin change the apparent habit of the initial twin.[14,15] It has been suggested that these factors can cause the double twin to end up parallel to a $\{30\bar{3}4\}$ plane,[15] which is inclined 7.3 deg to the original $\{10\bar{1}1\}$ plane. Twins parallel to these planes were therefore considered in the present analysis. An example (twin 17 in Figure 6) is shown in Figure 8. The traces of the $\{10\bar{1}2\}$, $\{10\bar{1}1\}$, and $\{30\bar{3}4\}$ planes were calculated and compared with the inclination of the observed twins. In all,

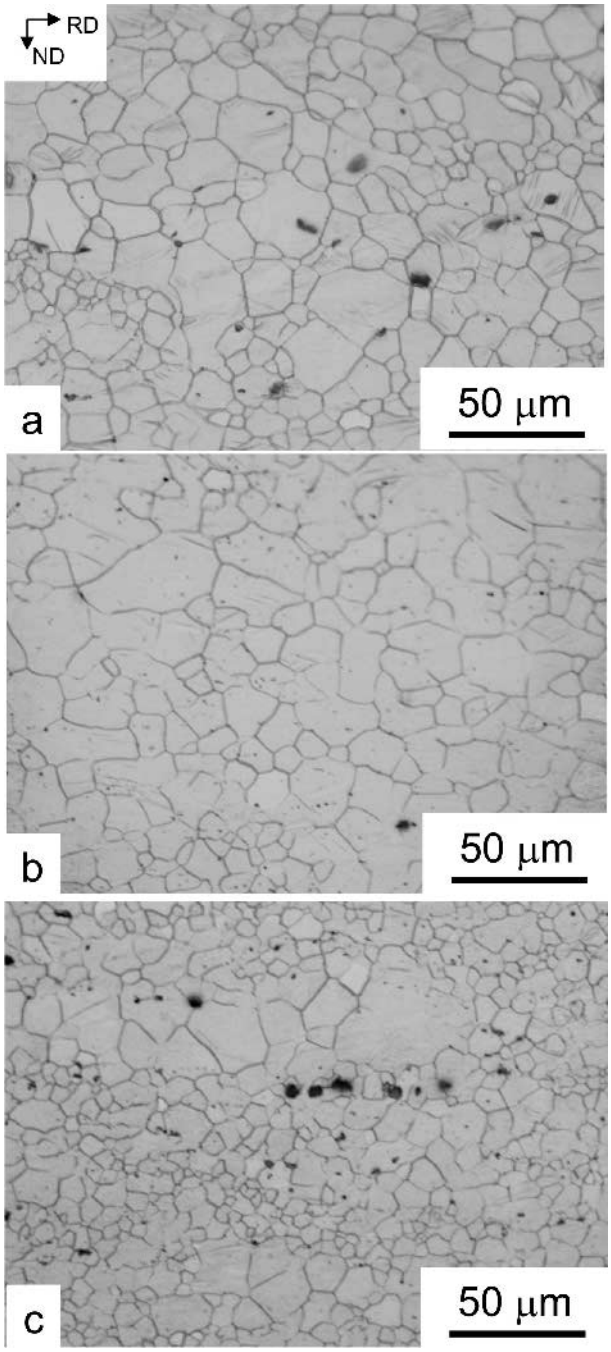

Fig. 4—Fully recrystallized structures after rolling to a total strain of 0.7 for (*a*) cast starting material rolled in six passes at 400 °C, (*b*) plate starting material rolled in six passes at 400 °C, and (*c*) plate starting material rolled in one pass at 400 °C. Each pass was followed by annealing at 400 °C for 15 min (RD-ND section, rolling direction parallel to scale marker).

43 twins were examined (Figure 6). Of these, 7 fell within 1 deg of a trace of a $\{10\bar{1}2\}$ plane, 17 fell within 3 deg of a trace of a $\{10\bar{1}1\}$ plane, and 16 fell within 3 deg of a trace of a $\{30\bar{3}4\}$ plane. The remaining three twins were within 5 deg of a $\{30\bar{3}4\}$ plane trace. The $\{10\bar{1}2\}$ twins identified from the trace analysis formed in grains oriented such that the rolling strain placed the *c*-axis in compression. An example of such a twin is given in Figure 9.

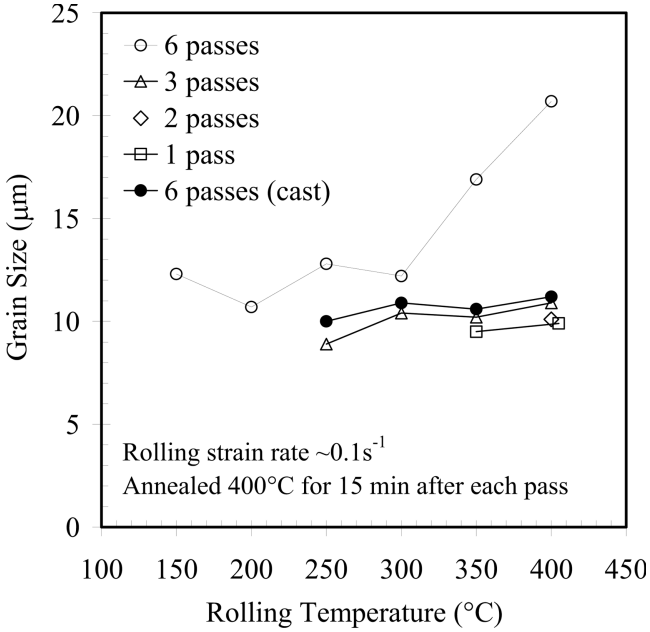

Fig. 5—Influence of rolling temperature on the grain size of the wrought samples following rolling and annealing. A subset of the cast data, for which near complete recrystallization occurred, is included for comparison. All samples were rolled to a total strain of 0.7.

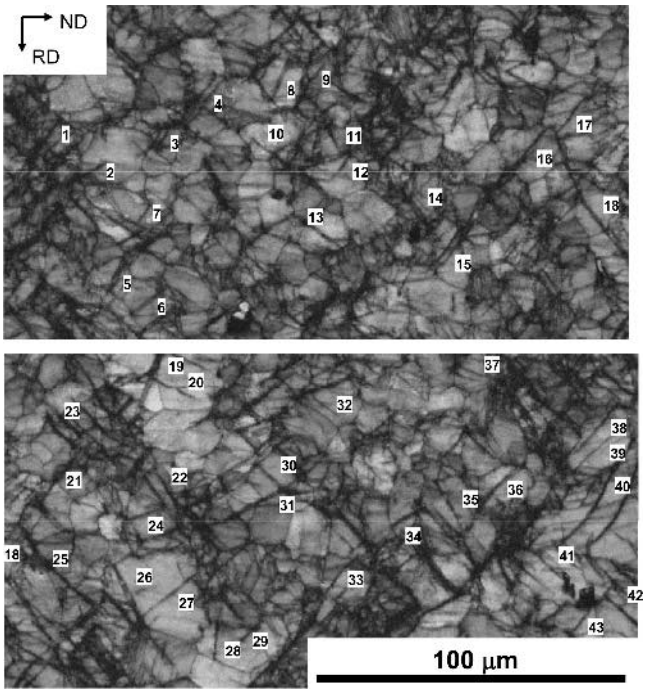

Fig. 6—Kikuchi band contrast map of the structure of AZ31 plate cold rolled to 15 pct reduction. The numbers are placed to the right of twins that were subjected to trace analysis.

C. *In-Situ Tensile Testing*

One explanation for the unexpected formation of $\{10\bar{1}2\}$ twins in grains oriented for *c*-axis compression is that these twins form during unloading. To explore this possibility, a series of *in-situ* EBSD observations of a sample of the cast AZ31 material were carried out using a tensile stage mounted

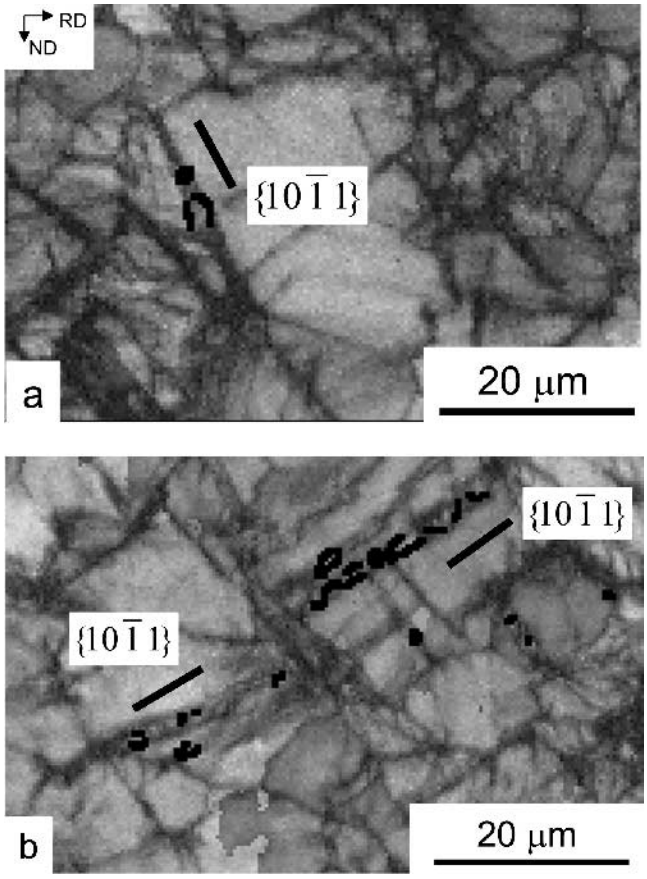

Fig. 7—Fragments of boundaries consistent with {10$\bar{1}$1}/{10$\bar{1}$2} double twinning. The Kikuchi band contrast is shown and boundaries within ±5 deg of a 38 deg rotation around a <11$\bar{2}$0> direction are marked in bold. The trace of the nearest {10$\bar{1}$1} plane to the twin is also given (AZ31 plate cold rolled 15 pct).

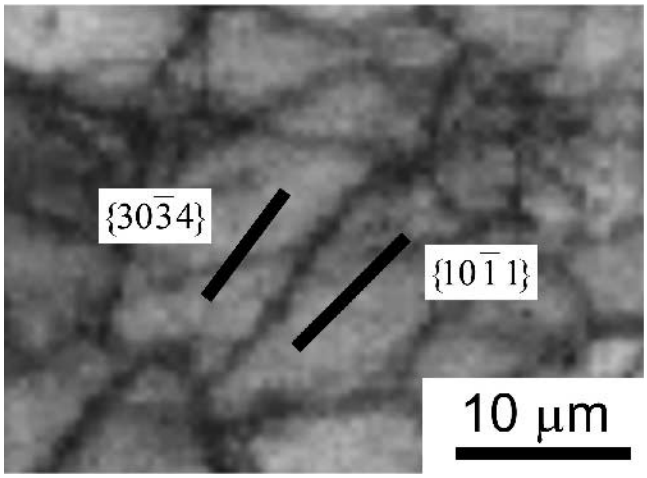

Fig. 8—A "close-up" of a dark linear feature assumed to be a twin (twin 17 from Fig. 6). The average habit of the feature is closer to a {30$\bar{3}$4} plane than a {10$\bar{1}$1} plane.

within a scanning electron microscope. Images corresponding to the starting structure, the structure in the loaded state following a strain of ~0.05, and the structure following unloading are shown in Figure 10. A number of interesting observations can be made.

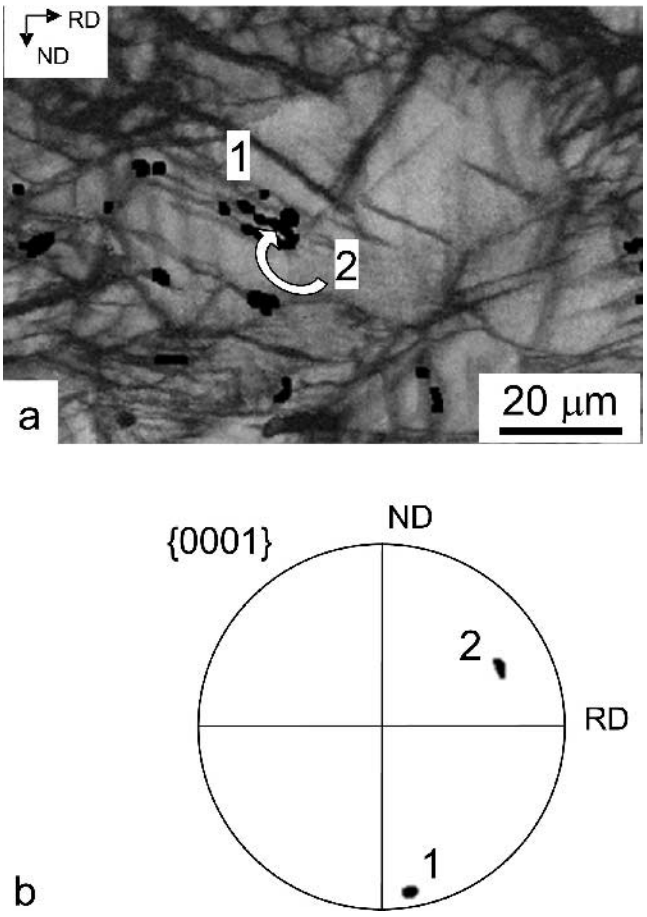

Fig. 9—Fragments of boundaries consistent with {10$\bar{1}$2} *c*-axis tension twinning: (a) Kikuchi band contrast with boundaries within ±5 deg of an 86 deg rotation around a <11$\bar{2}$0> direction marked in bold; and (*b*) pole figure showing the matrix (1) and twin (2) orientations (both images in RD-ND section, rolling direction horizontal).

(a) The application of strain to grain 3 resulted in the disappearance (from the observation plane and within the resolution of the EBSD measurement) of the {10$\bar{1}$2} twins present at the beginning of the test.
(b) The removal of the load resulted in the reappearance of {10$\bar{1}$2} twins in grain 3 but not to a degree significantly greater than originally present.
(c) The removal of the load resulted in a reduction in the size and number of twins in grain 2.
(d) The removal of the load resulted in the appearance of many twins in grain 6. No twins were apparent in the observation plane of this grain initially or in the loaded state.

Of main interest here is the last observation in that it indicates that {10$\bar{1}$2} twins can indeed grow, or possibly form, during unloading following deformation. The *c*-axis of the grain in which this was observed was aligned nearly perpendicular to the tensile axis. The twins that formed in this grain provide extension perpendicular to the tensile direction, in opposition to the imposed loading strain.

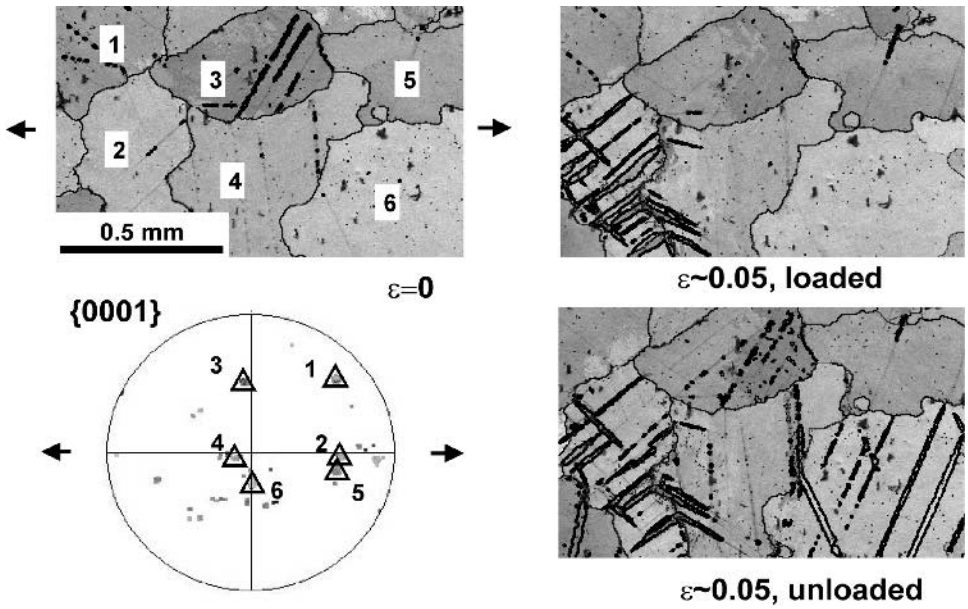

Fig. 10—Microstructures obtained during *in-situ* observation of a tensile test. The images show Kikuchi band contrast, high-angle grain boundaries, and $\{10\bar{1}2\}$ tension twins (in bold). The tensile direction is marked by the arrows.

IV. DISCUSSION

A. *Microstructures Following Hot Rolling*

There are two main observations arising from the examination of the hot-rolled microstructures: (1) that incomplete recrystallization occurred in most of the cast samples and (2) that enhanced grain refinement was seen at lower temperatures and higher pass strains in the fully recrystallized samples. The former is probably just a reflection of the fact that coarser grained materials recrystallize more slowly than fine-grained materials, due to the large role played by grain-boundary nucleation.[21] The present results suggest that this is best alleviated by repeated low strain passes rather than by an increase in the pass strain (at least for a total strain of 0.7). This can also be attributed to the important role played by grain boundaries in nucleating recrystallization. That is, in the present cast samples, the grain-boundary area available for nucleation can be considered to increase more by repeated steps of low strain rolling and annealing than by the application of high strain.

It is interesting to note that the boundaries of some of the grains deemed here to be unrecrystallized appeared to show signs of having "bulged" out into the neighboring fine-grained regions (Figure 2(a)). This may have resulted, in some cases, in an increase in the size of these grains. The elongated morphology and internal structure of many of these grains suggest that they are indeed retained deformed grains rather than grains produced by abnormal grain growth. Future work is required, however, to quantify the degree to which some form of abnormal growth might be playing a role.

The greater refinement in final grain size seen with decreasing rolling temperature is also a similar observation to that made in other metals[21] and can be rationalized in terms of an increased nucleation density caused by the finer deformation structures produced in lower temperature deformations.[21] Some grain refinement also occurred with increasing pass strain. This is also a common observation and can be ascribed to the increase in grain-boundary surface area and the refinement of the deformation structure that accompanies more severe deformations.

From a practical point of view, the effect of pass strain on grain size within the present range is not great, and it appears that as long as a pass strain of ~0.12 was employed (*i.e.*, that the present rolling strain of ~0.7 was achieved in six passes), further increases in pass strain for the sake of grain refinement would hardly be warranted. This seems to conflict with findings for other alloys quoted previously,[12,13] and the discrepancy may reside in the fact that the grains observed in the previous studies may well have been dynamically, rather than statically, recrystallized.

For rolling pass strains of ~0.12 and rolling temperatures >250 °C, finer recrystallized grains were achieved in the cast material than in the plate samples. This is difficult to understand. The roles of grain growth and particle pinning in the present work are unclear, and the interaction between these phenomena may play a role in determining the grain size. The faster recrystallization in the finer grain-sized plate samples may have left more time for grain growth to occur during annealing, but these are speculative ideas and more work is required to understand the factors controlling grain size.

Despite the apparent dominance of grain-boundary-nucleated recrystallization, evidence for intragranular nucleation was seen in the present work by way of recrystallized grains forming at twins. This has been reported previously[22,23] and is expected to arise, at least in part, from the provision of extra high-angle boundaries from which recrystallization nuclei can be formed. It is interesting to note, however, that the present work provides some evidence that the rate of migration of a recrystallizing front can be enhanced by twins, due either to the internal deformed structure or the surface energy of the boundaries. An example of apparently fast rates of growth along a twin is provided in Figure 11. In this figure, a recrystallized grain appears to have formed at the

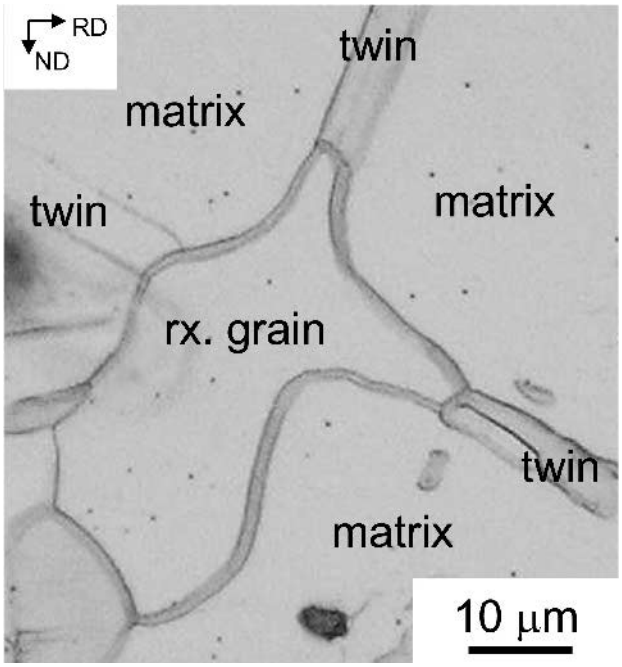

Fig. 11—Example of nucleation of recrystallization at twins in the cast starting material after rolling to a total strain of 0.7 in six passes at 200 °C with annealing at 400 °C for 15 min after each pass. The identification of the microstructural components is based on an inspection of the same region under lower magnifications.

intersection of two twins. The elongation of its boundary along the twins suggests a faster rate of growth in the twins.

B. *Twinning*

The trace analysis carried out here suggests that approximately three quarters of the twins examined were consistent with twins parallel to a $\{10\bar{1}1\}$ or $\{30\bar{3}4\}$ plane. However, the single image plane approach employed suffers from lack of knowledge of the inclination of the twins to the viewing plane. To help test the idea that these twins are indicative of the action of $\{10\bar{1}1\}$ twinning or $\{10\bar{1}1\}$-$\{10\bar{1}2\}$ double twinning, Schmid factors (SFs) were calculated for the relevant $\{10\bar{1}1\}$ twinning systems. In the case of the twins with a $\{30\bar{3}4\}$ habit, this was taken to be the nearest $\{10\bar{1}1\}$ twinning system. The SF was calculated by resolving an assumed macroscopic stress state of $\sigma_1 = 0$ and $\sigma_3 = 2\sigma_2$ onto the twin reference frame (which comprises the normal to the twin shear plane, the twin shear direction, and the direction orthogonal to these two directions). The SF values were then calculated by taking the ratio of the resolved shear stress on the twin plane and in the twin direction to the macroscopic normal stress in the rolling normal direction, σ_3.

Despite the crude nature of the SF approach, which ignores the local stress state, most of the SFs obtained in this analysis exceeded a value of 0.35. If twins with an SF lower than this value are excluded from the analysis, 63 pct of the twins examined are consistent with a $\{10\bar{1}1\}$ twinning system (Table I). This twinning mode (and its secondary twins) appears to be a significant deformation mechanism in the cold rolling of AZ31.

It is interesting to note that the twins spanning from twin 15 to twin 16 and from twin 17 to twin 18 in Figure 6 intersect the boundaries of their respective grains at points corresponding to where the twin in the neighboring grain intersects the same boundary. One interpretation of this is that the twinning events are coordinated in neighboring grains, something that may well be a precursor to the formation of bands of local deformation seen at higher strains.[3,6]

Table I. Data Collected from Trace Analysis of the 43 Twins Identified in Figure 6

Twin Type	Average Deviation from Ideal	Average SF	Fraction of Twins
$\{10\bar{1}1\}$	1.7 deg	0.43	37 pct
$\{30\bar{3}4\}$	1.6 deg	0.43	26 pct
$\{10\bar{1}2\}$	0.25 deg	"−ve"	16 pct
Excluded*	—	—	11 pct

*Twins with traces near $\{10\bar{1}1\}$ or $\{30\bar{3}4\}$ with an SF for $\{10\bar{1}1\}$ twinning <0.35.

The formation of $\{10\bar{1}2\}$ twins in opposition to the imposed strain was observed here, as it was in previous studies on pure Mg.[6,14] The SFs for the few $\{10\bar{1}2\}$ twins included within the twin trace analysis were all negative, in that they formed in grains oriented for *c*-axis compression. In light of the fact that $\{10\bar{1}2\}$ twins were observed to form during unloading in the present *in-situ* tensile tests, it is suggested that a similar mechanism operates in rolled material as it exits the roll bite. Reversal of twinning upon load reversal, "detwinning," has been discussed previously,[24] and the disappearance of $\{10\bar{1}1\}$ twins upon load removal has been suggested by Gharghouri *et al.*[25] The appearance of new $\{10\bar{1}2\}$ twins upon load removal, however, does not seem to have attracted much attention, although anecdotal reports of the phenomenon have been published.[14,26] Nevertheless, it can be speculated that they form during unloading in response to the inhomogeneity of the internal stress distribution. The role of these twins in subsequent mechanical and physical behavior is yet to be determined. It is also possible that a similar phenomenon accounts for unexpected $\{10\bar{1}2\}$ twins seen in zirconium tested in compression.[27]

V. CONCLUSIONS

1. Multipass hot rolling appears to be more effective at generating completely recrystallized structures than heavy pass rolling reductions. This is due to the dominance of grain-boundary nucleation of recrystallization. Intragranular nucleation of recrystallization at twins is nevertheless an important mechanism that may be able to be exploited in future wrought processing configurations.
2. Double twins in which $\{10\bar{1}1\}$ twinning is followed by $\{10\bar{1}2\}$ twinning were observed in cold-rolled Mg-3Al-1Zn, after 15 pct rolling reduction.
3. Approximately two thirds of the twins following 15 pct cold rolling had a trace parallel to either a $\{10\bar{1}1\}$ or a $\{30\bar{3}4\}$ plane and a SF for $\{10\bar{1}1\}$ twinning greater than 0.35.
4. *In-situ* EBSD analysis of room-temperature uniaxial tension testing demonstrated, qualitatively, that $\{10\bar{1}2\}$ "tension" twins can indeed grow (or possibly form) during unloading of AZ31. This phenomenon may explain the unexpected presence of these twins in cold-rolled Mg alloys.

ACKNOWLEDGMENTS

The authors thank Colleen Bettles, Rob McConville, Simon Jacob, Rob Pow, and John Vella for help with experimentation. This work was supported in part by the Australian Magneslium Corporation and the Australian Research Council.

REFERENCES

1. P. Menzen: in *The Technology of Magnesium and Its Alloys*, A. Beck, ed., F.A Hughes and Co. Ltd., London, 1940, p. 393.
2. S.L. Couling, J.F. Pashak, and L. Sturkey: *Trans. ASM*, 1959, vol. 51, pp. 94-107.
3. C.S. Roberts: *Magnesium and Its Alloys*, John Wiley, New York, NY, 1960, pp. 81-107.
4. M.T. Perez-Prado, J.A. del Valle, and O.A. Ruano: *Scripta Mater.*, 2004, vol. 50, pp. 667-71.
5. F. Kaiser, J. Bohlen, D. Letzug, K.U. Kainer, A. Styczynski, and C. Hartig: *Proc. 6th Int. Conf. Magnesium Alloys and Their Applications*, K.U. Kainer, ed., Wiley-VCH, Weinheim, 2004, pp. 456-62.
6. M.R. Barnett, M.D. Nave, and C.J. Bettles: *Mater. Sci. Eng. A,* 2004, vol. 386*,* pp. 205-11.
7. N. Ono, K. Nakamura, and S. Miura: *Mater. Sci. Forum*, 2003, vols. 419–422, pp. 195-200.
8. R. Kawalla, N. Coung, and A. Stolnikov: *Proc. 6th Int. Conf. on Magnesium Alloys and Their Applications*, K.U. Kainer, ed., Wiley-VCH, Weinheim, 2004, pp. 803-10.
9. R.K. Nadella, I. Samajdar, and G. Gottstein: *Proc. 6th Int. Conf. on Magnesium Alloys and Their Applications*, K.U. Kainer, ed., Wiley-VCH, Weinheim, 2004, pp. 1052-57.
10. Y.-H. Chen, S. Lee, and J.-Y. Wang: *Mater. Sci. Forum*, 2003, vols. 419–422, pp. 383-86.
11. G. Itoh, Y. Iseno, and Y. Motohashi: *Mater. Sci. Forum*, 2003, vols. 419–422, pp. 355-58.
12. J.A. Del Valle, M.T. Perez-Prado, and O.A. Ruano: *Mater. Sci. Eng. A*, 2003, vol. 355, pp. 68-78.
13. A. Galiyev, R. Kaibyshev, and D. Voronin: *Proc. 6th Int. Conf. Magnesium Alloys and Their Applications*, K.U. Kainer, ed., Wiley-VCH, Weinheim, 2004, pp. 266-71.
14. B.C. Wonsiewicz and W.A. BackoFen: *Trans. AIME,* 1967, vol. 239, pp. 1423-31.
15. W.H. Hartt and R.E. Reed-Hill: *Trans. AIME*, 1967, vol. 239, pp. 1511-17.
16. M.D. Nave and M.R. Barnett: *Scripta Mater.*, 2004, vol. 51, pp. 881-85.
17. M.H. Yoo and J.K. Lee: *Phil. Mag. A*, 1991, vol. 63, pp. 987-1000.
18. G.E. Dieter: in *Mechanical Metallurgy*, McGraw-Hill, Singapore, 1988, p. 611.
19. K. Pettersen and N. Ryum: *Metall. Trans. A*, 1989, vol. 20A, pp. 847-52.
20. *HKL "CHANNEL 5" Software Manual*, HKL Technology, Denmark, 2003.
21. F.J. Humphreys and M. Hatherly: *Recrystallization and Related Annealing Phenomena*, Elsevier, Oxford, United Kingdom, 1996, pp. 173-200.
22. R.O. Kaibyshev and O.S. Sitdikov: *Phys. Met. Metallogr.*, 2000, vol. 89, pp. 384-90.
23. M.M. Myshlyaev, H.J. McQueen, A. Mwembela, and E. Konopleva: *Mater. Sci. Eng. A*, 2002, vol. 337, pp. 121-33.
24. R.L. Woolley: *J. Inst. Met.*, 1954, vol. 83, pp. 57-58.
25. M.A. Gharghouri, G.C. Weatherly, J.D. Embury, and J. Root: *Phil. Mag.*, 1999, vol. 79, pp. 1671-95.
26. F.E. Hauser, C.D. Starr, L. Tietz, and J.E. Dorn: *Trans. ASM*, 1955, vol. 47, pp. 102-33.
27. T.A. Mason, J.F. Bingert, G.C. Kaschner, S.I. Wright, and R.J. Larsen: *Metall. Mater. Trans. A*, 2002, vol. 33A, pp. 949-54.